Macromolecules

Article

Connecting the Stimuli-Responsive Rheology of Biopolymer Hydrogels to Underlying Hydrogen-Bonding Interactions

Giulia Giubertoni, Federica Burla, Huib J. Bakker,* and Gijsje H. Koenderink*

Cite This: Macromolecules 2020, 53, 10503−10513

Read Online

ACCESS | Metrics & More | Article Recommendations | Supporting Information

ABSTRACT: Many biopolymer hydrogels are environmentally responsive because they are held together by physical associations that depend on pH and temperature. Here, we investigate how the pH and temperature responses of the rheology of hyaluronan hydrogels are connected to the underlying molecular interactions. Hyaluronan is an essential structural biopolymer in the human body with many applications in biomedicine. Using two-dimensional infrared spectroscopy, we show that hyaluronan chains become connected by hydrogen bonds when the pH is changed from 7.0 to 2.5 and that the bond density at pH 2.5 is independent of temperature. Temperature-dependent rheology measurements show that because of this hydrogen bonding the stress relaxation at pH 2.5 is strongly slowed down in comparison to pH 7.0, consistent with the sticky reptation model of associative polymers. From the flow activation energy, we conclude that each polymer is cross-linked by multiple (5−15) hydrogen bonds to others, causing slow macroscopic stress relaxation, despite the short time scale of breaking and reformation of each individual hydrogen bond. Our findings can aid the design of stimuli-responsive hydrogels with tailored viscoelastic properties for biomedical applications.
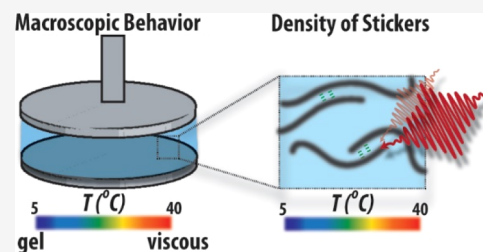
INTRODUCTION

Hydrogels are an appealing class of polymer materials because of their responsiveness to environmental stimuli such as temperature, pH, and ionic strength.[1] Hydrogels derive this responsiveness from the presence of reversible associations between the constituent polymer chains, such as electrostatic, hydrogen-bonding, or hydrophobic associations or metal complexation.[2] Stimuli-responsive hydrogels have a wide range of applications, such as adhesives,[3] controlled drug delivery,[4] surrogate extracellular materials for tissue regeneration,[5] and bioinks for printing of soft tissues.[6]

For biomedical applications, it is advantageous to create hydrogels from biopolymers that are naturally present in the human body, as these can capture both the mechanical and biological properties of the extracellular environment.[5] A particularly interesting biopolymer in this context is hyaluronan because of its ubiquity in human tissues and extracellular fluids such as the synovial fluid in joints and the vitreous humor of the eye.[7,8] Hyaluronan is a linear polyelectrolyte composed of repeating units of D-glucuronic acid and N-acetyl-D-glucosamine joined by glycosidic bonds.[9,10] In healthy tissues, hyaluronan has a very high molecular weight of up to 10 MDa, corresponding to chain lengths of tens of micrometers.[11] Its length combined with its anionic nature enable hyaluronan to form soft hydrated viscoelastic fluids.[12−14] These properties are at the basis of hyaluronan's roles in the lubrication of joints[15] and in tuning the transport properties and mechanical response of tissues such as skin, cartilage, and brain.[16,17] Hyaluronan's mechanical properties together with its biochemical interactions regulate cell−matrix and cell−cell interactions, thus influencing cell−cell communication,[18] wound healing,[19] and angiogenesis and development.[20] Accordingly, abnormalities in the expression level or molecular weight of hyaluronan brought about by aging or genetic disorders contribute to various diseases, such as inflammation,[21] multiple sclerosis,[22] cancer[23,24] and cartilage degeneration.[25]

Because of its central importance to human health and disease, there have been many studies of the material properties of isolated hyaluronan (reviewed in ref 14). Like many other biological polyelectrolytes, hyaluronan is responsive to external stimuli, such as temperature, solution pH, salt concentration, and multivalent counterions.[9,26,27] Of these triggers, the solution pH has the most marked effect: in a narrow pH range centered around pH 2.5, hyaluronan solutions turn into soft solids that are stretchable.[28−31] This special gel state is sometimes referred to as the *putty* state.[32] We recently showed with two-dimensional infrared (2DIR) spectroscopy that this gelation process is caused by the pH-dependent formation of specific interchain hydrogen bonds between the carboxyl and amide groups on adjacent chains (see Figure 1a).[33]
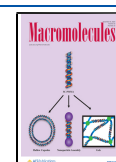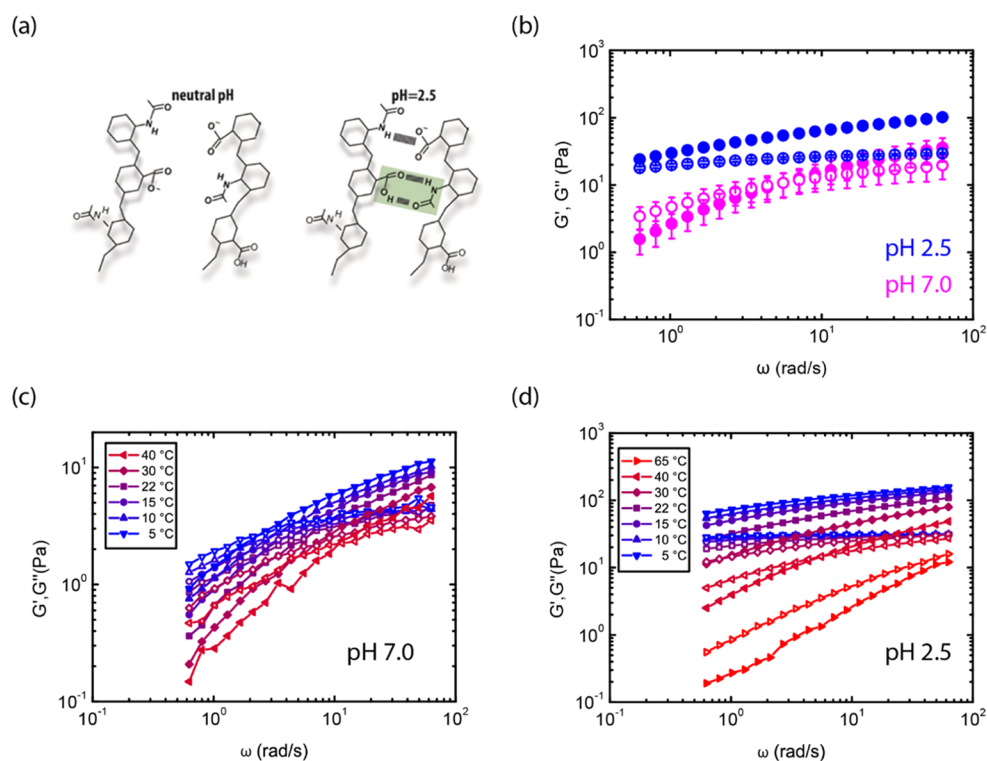
Figure 1. (a) Schematic showing the linear structure of hyaluronan, consisting of repeating disaccharides composed of *N*-acetyl-glucosamine and glucuronic acid. At neutral pH (pH 7), the deprotonated carboxyl groups confer a net negative charge. At pH 2.5, the chains associate by the formation of hydrogen bonds between the carboxylic acid, the deprotonated carboxylate anion, and the amide groups of the hyaluronan polymers.[39] (b) Frequency spectra of the linear viscoelastic shear moduli of hyaluronan hydrogels (*c* = 10 mg/mL) at room temperature (*T* = 22 °C) at pH 7.0 (pink) and pH 2.5 (blue). Symbols denote the elastic (solid circles) and viscous (open circles) shear moduli. (c) Temperature dependence of the frequency spectra of the shear moduli of hyaluronan solutions at pH 7.0. (d) Corresponding frequency spectra at pH 2.5. Note that curves in Figure 1b represent an average over three different repeats, while Figure 1c,d shows one representative repeat at each temperature.

2DIR spectroscopy is uniquely capable of directly probing molecular interactions by measuring vibrational interactions using an intense femtosecond pump laser to excite the vibrations and a weaker probe beam to measure the induced vibrational responses. We found that at neutral pH all the carboxyl groups are deprotonated, and thus associative interactions between different polymer chains are prohibited by strong electrostatic repulsion. Hence, at neutral pH, the mechanical properties of hyaluronan solutions are dictated by chain entanglements. By lowering the pH to 2.5, close to the isoelectric point of hyaluronan[33] of ~2.9, around 80% of the carboxyl groups are protonated. Protonation weakens the repulsive electrostatic forces between the chains and at the same time provides protonated carboxyl groups that participate in the formation of double hydrogen bonds, together with amide groups and carboxylate anion groups (Figure 1a).

The material properties of responsive hydrogels can be tuned via the lifetime of the reversible cross-links and their number density. There are several theoretical models for associative polymers that predict how the viscoelastic behavior depends on the cross-linker lifetime and density,[34,35] but it remains challenging to understand the connection between macroscopic and molecular time scales. Hydrogen bonds tend to be short-lived, forming and breaking on a timescale of a few to tens of picoseconds.[36] Macroscopic stress relaxation in hyaluronan gels at pH 2.5 occurs on much longer time scales, ranging up to minutes. Here, we study the impact of temperature and pH on the rheology of hyaluronan hydrogels and on the underlying hydrogen-bond-mediated cross-linking

by combining rheology and 2DIR spectroscopy. We compare hyaluronan at neutral pH, where the chains interact by excluded volume interactions (i.e., topological entanglements) only,[26,37,38] and at pH 2.5, where the chains additionally interact by transient hydrogen-bond associations.[39] We use time−temperature superposition (TTS) rheology to measure the time scale and activation energy for network flow and interpret these findings in the context of the sticky reptation model[34,35] previously applied to entangled synthetic polymers interacting by thermoreversible cross-linking.[40,41] We use 2DIR spectroscopy to directly measure the density of interchain hydrogen bonds as a function of temperature.

■ EXPERIMENTAL SECTION

Materials and Sample Preparation. Hyaluronan sodium salt in powder form obtained by fermentation of *Streptococcus equii* with a nominal molecular weight of 1.5−1.8 MDa was obtained from Sigma-Aldrich. This molecular weight corresponds to a chain length of 3−4 *μ*m and about 3750 disaccharides (considering that the disaccharide units have a molecular weight of 400 Da and a length of ~1 nm [ref 42]). For rheological measurements, solutions of high molecular weight hyaluronan with concentrations between 5 and 20 mg/mL were prepared by dissolving accurately weighed amounts of hyaluronic acid in an aqueous solution containing 0.15 M NaCl (Sigma-Aldrich) and HCl (Sigma-Aldrich) ranging from 0 to 40 mM. The solution pH was measured with a pH meter equipped with a microelectrode (Hanna Instruments, Germany). The samples were left to equilibrate at room temperature for at least 24 h before measuring. Samples were stored for at most 1 week at a temperature of 4 °C. For the spectroscopic experiments, solutions of high molecular weight hyaluronan in the putty state were prepared by

dissolving 20 mg/mL hyaluronan sodium salt in heavy water (D_2O) at a DCl concentration of 40 mM, which was previously determined to be the correct concentration to obtain the pH = 2.5 putty state conditions.[39] We dissolved hyaluronan in D_2O to facilitate the infrared observation of the amide and carbonyl stretch vibrations, which carry the structural information, at wavenumbers around 1630 and 1720 cm^{-1}, respectively. Infrared measurements cannot be performed in H_2O solutions, as the amide and carbonyl vibrations of hyaluronic acid absorb in the same infrared frequency region as the bending vibration of H_2O (between 1600 and 1700 cm^{-1}). The bending vibration of D_2O is instead strongly red-shifted to 1200 cm^{-1}.[43] Note that the pD value of a D_2O solution can be converted to the pH value of an H_2O solution of similar acidity using pH = pD*0.929.[44]

TTS Rheology Experiments. We measured the frequency spectra of the linear viscoelastic shear moduli as a function of temperature with a stress-controlled MCR 501 rheometer (Anton Paar, Austria) using a plate−plate measuring geometry with a 40 mm diameter and 100 μm gap. The plate temperature was controlled by a Peltier plate connected to the lower plate and a hood controlling the temperature of the upper plate. Samples were loaded at room temperature (22 °C) and equilibrated for 10 min before starting the experiments. Small amplitude (0.5% strain) oscillatory shear tests were performed at 20 frequencies logarithmically spaced between 0.1 and 10 Hz, at temperatures of 5, 10, 15, 22, 30, and 40 °C. We started at 22 °C and first decreased the temperature to 15, 10, and 5 °C and then increased the temperature to 30 and 40 °C. The temperature was adjusted between each frequency sweep at the fastest rate allowed by the rheometer (around 2 °C/s), and after reaching the desired temperature, we waited for equilibration by waiting for the elastic and loss moduli to saturate, which always occurred within 2 min. We verified that there was no hysteresis in the viscoelastic moduli upon cooling back to 22 °C until we increased the temperature to 60 °C (Figure S1), consistent with prior work,[45] that showed that hyaluronan is stable up to 50 °C and is hydrolyzed above 90 °C on a timescale of ~1 h. TTS analysis of the frequency (ω) spectra was performed by determining the shift factor $a_T(T)$ required to overlap both the elastic modulus $G'(\omega)$ and the viscous shear modulus $G''(\omega)$ with their respective reference curves measured at the reference temperature T_0 = 295 K (22 °C). The temperature dependence of the shift factors $a_T(T)$ was fitted to an Arrhenius equation to obtain the activation enthalpy E_a for stress relaxation

$$\log(a_T) = -\frac{E_a}{2.303R}\left(\frac{1}{T} - \frac{1}{T_0}\right) \tag{1}$$

where R is the universal gas constant. The activation energy in units of k_BT is obtained by dividing by Avogadro's number, where k_B is Boltzmann's constant and T is the absolute temperature. At each temperature, we performed experiments on three independently prepared samples.

Linear Infrared Spectroscopy (FTIR). We measured Fourier Transform Infrared (FTIR) spectra of the samples with a Bruker Vertex 80v FTIR spectrometer equipped with a liquid-nitrogen-cooled mercury−cadmium−telluride (MCT) detector. The spectra were recorded under a nitrogen atmosphere at a wavenumber resolution of 3 cm^{-1}. We averaged 100 scans for every spectrum. In all measurements, we used a standard sample cell with a path length of 100 μm. The temperature-dependent FTIR spectra were measured with the aid of a Peltier-cooled temperature cell (Mid-IR Falcon, Pike technologies). The temperature was ramped from 20 to 40 °C at a rate of 1 °C/min. The spectra were corrected for the absorption of the D_2O solvent background at the same temperature. These background spectra were measured using the same ramping parameters. To determine if the ratio between the two protonation states of the carboxyl group depends on temperature, we fitted the linear infrared spectra measured at different temperatures using a global fitting procedure. This fit is based on the minimization of the square error

$$\sum_{i,j}(S(\omega_j, T_i) - S^{exp}(\omega_j, T_i))^2 \tag{2}$$

where S is the fitted spectrum, S^{exp} is the experimental spectrum, ω_j is the frequency, and T_i is the temperature. Assuming that the vibrational bands are Gaussian shaped, we expect that

$$\forall\, i,\; \text{for } \omega_{\{min\}} \leq \omega_j \leq \omega_{\{max\}}$$

$$S(\omega_j, T_i) = \sum_{k=1,2,3} c_k(T_i)g_k(\omega_j) + c_{bk}(T_i)S_{bk}(\omega_j) \tag{3}$$

where g_k represents the three Gaussians that describe the absorption bands of the antisymmetric stretching mode of the carboxylate anion (COO_{ant}^-), the amide I mode (AM.I), and the carbonyl stretching mode of the protonated carboxyl group (C=O), respectively, and c_k represents the Gaussians amplitudes. $S_{bk}(\omega_j)$ represents the spectrum used for background correction. Based on previous work,[39] the Gaussians were centered at 1609, 1634, and 1725 cm^{-1} for the absorption bands of the COO_{ant}^-, AM.I and C=O vibrations, respectively. To account for the fact that increasing the temperature leads to a slight shift of the absorption bands,[46] the center frequencies were allowed to shift by a maximum of 1 cm^{-1} when fitting the linear spectrum at 40 °C. The widths of the three bands are global parameters in the fit, meaning that they are fixed at all studied temperatures and only the amplitudes of the three bands are allowed to be different at each temperature. We can then find the areas of the COO_{ant}^-, AM.I, and C=O absorption bands at each temperature, and compare their ratio at different temperatures.

2DIR Spectroscopy. 2DIR measurements were performed using a home-built setup described elsewhere.[47] We excite the amide and carboxyl vibrations with a pair of strong femtosecond mid-infrared pulses centered at 1670 cm^{-1} with a bandwidth of 200 cm^{-1} (~100 fs, 4 μJ per pulse). This excitation induces transient absorption changes that we probe with a weaker (0.35 μJ) single femtosecond probing pulse that is delayed by a waiting time T_w. After propagation through the sample, the probe pulse was sent into an infrared spectrograph and detected with an infrared MCT detector array, thus yielding the transient absorption spectrum as a function of the probe frequency. The dependence of the transient absorption spectrum on the excitation frequency was determined by measuring transient spectra for many different delay times τ between the two excitation pulses. By Fourier transformation of these spectra, we obtain the dependence of the transient absorption spectrum on the excitation frequency. By plotting the transient absorption spectrum as a function of the excitation and the probing frequency, we obtain 2DIR transient absorption spectra for each delay time T_w between the excitation and probing pulses. The temperature of the sample was kept constant during the experiment with a Peltier element with an active feedback loop.

■ RESULTS AND DISCUSSION

pH Dependence of Hyaluronan Hydrogel Rheology. To study the impact of pH-dependent cross-linking on hyaluronan hydrogel rheology, we compare solutions of hyaluronan polymers at pH 2.5 and pH 7.0 (see Figure 1a). These pH values were chosen because they represent two distinct regimes of hyaluronan chain interactions. At pH 7.0, previous rheology[37] and self-diffusion[26] measurements showed that hyaluronan chains interact by excluded volume interactions only, provided that the ionic strength of the solution is sufficiently high to screen the electrostatic repulsions of the chains. Nuclear magnetic resonance (NMR) and 2DIR[33] measurements,[48] compression measurements by atomic force microscopy (AFM),[49] and molecular dynamic simulations of hyaluronan[50] all showed that under neutral conditions, only intramolecular, no intermolecular, associative interactions are present. Specifically, NMR and
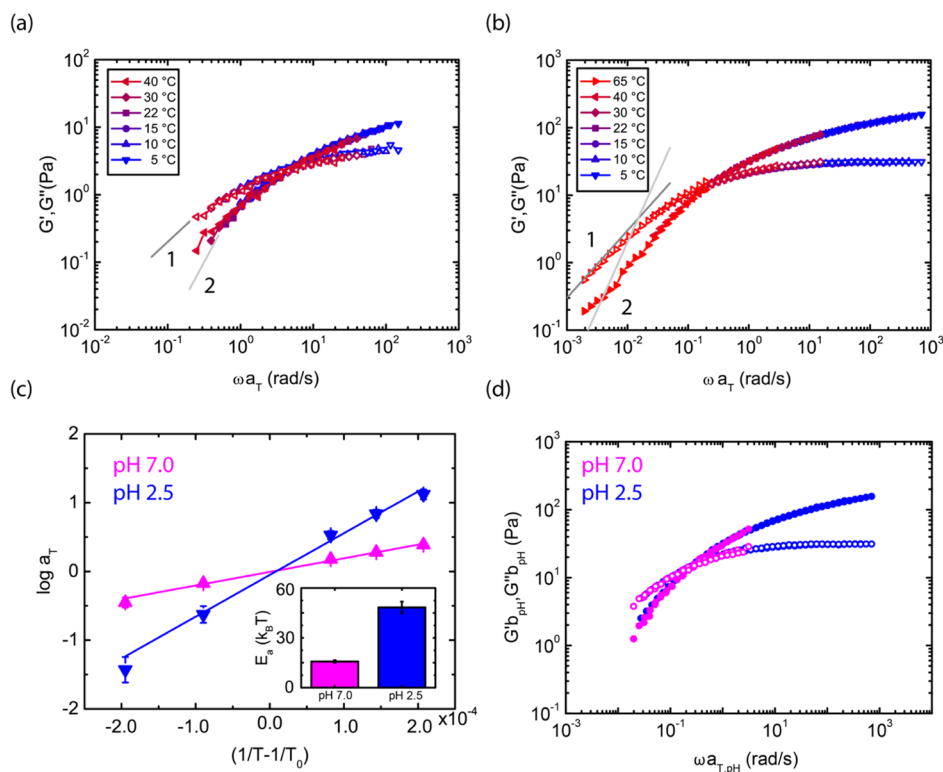
Figure 2. TTS rheology of hyaluronan solution (10 mg/mL). (a) Frequency sweeps at pH 7.0 obtained at different temperatures are shifted along the frequency axis onto the measurement at the reference temperature of 22 °C by multiplication with a shift factor a_T. (b) Corresponding rescaled frequency sweeps at pH 2.5. The gray lines in (a,b) indicate the expected terminal relaxation $G'' \propto \omega^1$ and $G' \propto \omega^2$ for a Maxwell fluid. (c) Arrhenius plot showing the shift factors used for constructing the TTS data as a function of the inverse of the temperature relative to the reference temperature. Lines show linear fits whose slopes represent the flow activation energy divided by 2.3R. Inset: Activation energies retrieved from the Arrhenius fits, expressed in units of thermal energy $k_B T$. (d) Universal master curve for hyaluronan hydrogel rheology obtained by rescaling all frequency sweeps gathered at different temperatures (5 and 40 °C, not color-coded) and pH values (2.5 and 7.0, see legend) onto a reference set measured at pH 2.5 and at 22 °C (blue triangles). We first shifted the horizontal axis and then the vertical axis to obtain overlap.

molecular dynamics simulations showed that a set of specific intramolecular hydrogen bonds, involving the hydroxyl groups of the sugar rings, is formed, increasing the chain stiffness of hyaluronan.[48,50,51] Additionally, a small fraction (~10%) of carboxyl and amide groups of adjacent units form intramolecular hydrogen bonds.[33] However, based on 2DIR experiments performed at different temperatures, we previously concluded that such intrachain interactions do not significantly contribute to the polymer rigidity.[33] At pH 7, there is no experimental evidence of the presence of interchain associative interactions.[48] This molecular picture is also in line with several macroscopic studies, which showed that hyaluronan chain dynamics is dependent only on excluded volume interactions at pH 7.[52] At pH 2.5, high molecular weight hyaluronan forms soft and stretchable gels that are referred to as *putty*.[32,53] We recently showed with 2DIR spectroscopy measurements that this gel formation is driven by the pH-dependent formation of hydrogen bonds involving carboxylic acid, the deprotonated carboxylate anion, and the amide groups of adjacent hyaluronan chains (Figure 1a).[39] We performed the rheology experiments on samples with a polymer concentration of 10 mg/mL, in the *semidilute entangled* concentration regime. In this regime, the polymers experience transient topological constraints as a result of their high density.[14] The entangled regime sets in at the entanglement concentration c_e, which is generally a factor 2–5 higher than the overlap concentration c^*, where the polymer coils first touch.[54] For hyaluronan with a molecular weight of

1.5–1.8 MDa, $c^* \approx 2$ mg/mL.[55,56] We characterized the time-dependent rheology of the samples by performing frequency sweeps using strain oscillations with a small (0.5%) amplitude.

As shown in Figure 1b, the frequency spectra show a transition from a solid response (storage shear modulus G' larger than the loss modulus G'') at high frequencies to a fluid response ($G' < G''$) at low frequencies. This behavior is characteristic for entangled polymer solutions, where chains diffuse by reptation, that is, highly restricted diffusion because of entanglements with surrounding chains.[54] Entangled polymer solutions generally display a Maxwell-type behavior with a rubber-like plateau that persists down to a frequency $\omega \approx 1/\tau$ and a terminal ($\omega < 1/\tau$) regime, where the moduli tend toward $G'' \propto \omega^1$ and $G' \propto \omega^2$ scaling.[54] The main effects of lowering the pH are first a downshift of the frequency, where G' and G'' crossover, which marks the transition from the rubber plateau to the terminal regime (from 5 rad/s at pH 7.0 to ~0.2 rad/s at pH 2.5) and second an approximately 10-fold increase of the elastic modulus. The rheology data do not reach high enough frequencies to access the plateau regime but indicate approximate values for the plateau modulus of ~20 Pa at pH 7.0 versus ~200 Pa at pH 2.5. These changes are as expected for entangled polymers that experience transient cross-linking interactions, as formulated by the *sticky reptation* model.[34,35] This model predicts that sticky interactions slow down reptation by adding an additional friction on the chains that increases linearly with the (effective) bond lifetime and quadratically with the number of stickers per chain. The model

further predicts that transient cross-links enhance the shear modulus G_0 in the rubbery plateau because G_0 is proportional to the number density of elastically active network strands $\nu_x = cN_A/M$, according to $G_0 = \nu_x k_B T$. Here, N_A is Avogadro's number and M is the chain molecular weight. The magnitude of the elastic modulus is in line with what we expect at the hyaluronan concentration used here, which is just at the onset of entanglements ($c = 5c^*$[54]). The plateau modulus G_N of an entangled solution can be estimated according to $M_e = cRT/G_N$, where c is the polymer concentration and M_e is the entanglement or transient cross-linking molecular weight. We measure G_N values of around 20 Pa at pH 7.0 and 200 Pa at pH 2.5. We caution that these values are approximations, as the rheology data do not access high enough frequencies such that the elastic modulus has truly reached its plateau value. By using $R = 8.3\,[\text{Pa}][\text{m}^3][\text{K}^{-1}][\text{mol}^{-1}]$, $c = 10\,[\text{mg/mL}] = 104[\text{g/m}^3]$, $T = 293\,[\text{K}]$, we therefore estimate $M_e = 1.2 \times 10^6$ and 1.2×10^5 g/mole at pH 7.0 and 2.5, respectively. At pH 7, M_e is close to the average molecular weight (1.5–1.8 MDa) of the polymers. At pH = 2.5, we compute a ratio $M/M_e \approx 12-15$, indicating around 11–14 effective cross-links per chain.

Temperature Dependence of Hyaluronan Hydrogel Rheology. Our findings suggest that the rheology of hyaluronan hydrogels is controlled by a single time scale, which is modulated by pH-dependent chain interactions. To test this hypothesis, we performed measurements at different temperatures because temperature is known to change the time scale of hydrogen-bond breaking and reformation.[57] As shown in Figure 1c,d, the shear moduli both at neutral (pH 7.0) and at acidic (pH 2.5) hyaluronan solutions strongly depend on temperature. Increasing the temperature lowers the magnitude of the shear moduli and increases the characteristic frequency at which the rubber plateau crosses over to the terminal regime, consistent with faster stress relaxation. We note that the hyaluronan hydrogels were thermoreversible: there was no hysteresis in the rheology when the temperature was shifted back up or back down (Figure S1 in the Supporting Information).

To test whether a single interaction mechanism can indeed account for the observed temperature dependence, we performed a TTS analysis using 22 °C as the reference temperature. The idea behind this analysis is that the stress relaxation time according to the sticky reptation model is proportional to the (effective) bond lifetime and should therefore be exponentially dependent on temperature.[58] As shown in Figure 2, we can indeed construct master curves for both the pH 7.0 data set (Figure 2a) and the pH 2.5 data set (Figure 2b) by in each case shifting the data along the frequency axis by a temperature-dependent shift factor a_T. The fact that the same horizontal shift factors apply for G' and G'' indicates that hyaluronan gels are thermorheologically simple materials[47] for which a single temperature-dependent inter-action scale determines the rheology. The fact that we do not need any vertical (modulus) shift factor to superpose the frequency-dependent G'/G'' curves suggests that the equilibrium density of cross-links does not change appreciably with temperature. The modulus depends on temperature through two effects, namely, through a direct linear proportionality with $k_B T$ and through any temperature dependence of the cross-link density. Over the temperature range studied here (5–40 °C), the $k_B T$ term increases by only a factor of 1.1. Thus, the observation that we do not need a vertical shift indicates that the change in number density of interchain hydrogens bonds

with increasing temperature, if any, must be very small. The master curves clearly show Maxwell-type behavior with a rubbery plateau at the higher frequencies and a crossover to a terminal relaxation regime at lower frequencies. At pH 7.0, we do not reach sufficiently low frequencies to confirm whether the moduli at low frequencies tend toward the $G'' \sim \omega^1$ and $G' \sim \omega^2$ dependencies expected for a Maxwell fluid with a single relaxation time. At pH 2.5, we do reach lower normalized frequencies, but the low-frequency scaling of G' seems somewhat shallower than the $G' \sim \omega^2$ scaling of the Maxwell model. A likely explanation is the size polydispersity of the hyaluronan, which is known to cause broadening of the frequency spectrum of entangled polymers,[54] especially in the case of sticky polymers.[41]

To retrieve the pH dependence of the flow activation energy, we constructed Arrhenius plots of the shift factors a_T as a function of the inverse temperature relative to the reference temperature $T_0 = 22$ °C, both for pH 7.0 and pH 2.5.[59] As shown in Figure 2b, we obtained straight lines at both pH values, indicating that the relaxation time is controlled by the thermally activated dissociation of bonds between chains. As shown in Figure 2c, the activation energy at pH 2.5 (taken from the slope of the Arrhenius plots) is much higher than at pH 7.0, consistent with the expectation from the sticky reptation model that the formation of hydrogen bonds between the chains enhances the friction on the chains. In the entangled state at pH 7.0, the activation energy is around 12 $k_B T$ (or 30 kJ/mol), consistent with prior findings.[56] We note that the earlier work was carried out at 50 mg/mL, a much larger concentration than studied here (10 mg/mL), suggesting little effect of concentration on the activation energy. We also find little dependence of the activation energy on hyaluronan concentration at pH 7.0 when we extend the concentration range down to 5 mg/mL (see Figure S2). For the putty state at pH 2.5, the activation energy is much higher and amounts to $\sim 50 k_B T$ (or 115 kJ/mol). We measured similar activation energies at other hyaluronan concentrations (5–20 mg/mL) (see Figure S2). The much higher flow activation energy at pH 2.5 compared to pH 7.0 is consistent with the additional presence of transient associations between the chains.

Until now, we rescaled the data sets for different pH values onto separate master curves. To test if a single constitutive law describes all data, independent of pH and temperature, we finally rescaled all curves onto a single master curve. This idea was inspired by recent studies showing that TTS can be extended to other environmental parameters that control the relaxation times of noncovalent gels such as ionic strength.[60,61] We can indeed rescale the G' and G'' curves measured at pH 7.0 and pH 2.5 onto a single universal set of master curves, using in addition to the horizontal shift factor a_T for the frequency axis also a vertical shift factor $b_T \approx 1.5$. The collapse onto a single set of master curves strongly suggests that the physical mechanism that controls the rheology is the same, regardless of temperature and pH.

Spectroscopic Measurement of the Density of Intermolecular Interactions. Prior 2DIR spectroscopy measurements from our laboratory[39] showed that the cross-links between hyaluronan chains are formed by hydrogen bonds between the carboxylic acid, deprotonated carboxylate anion, and amide groups of adjacent hyaluronan polymers (Figure 1a). The cross-link density thus likely depends on the degree of protonation of the carboxyl groups, which could in

principle change with temperature. To test whether the protonation state of hyaluronan changes with temperature, we measured linear infrared absorption spectra of a solution of hyaluronan dissolved in D_2O at 20 and 40 °C (Figure 3). The
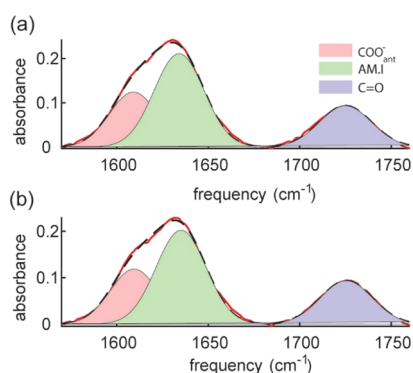

Figure 3. (a,b) Linear infrared spectra for a solution of hyaluronan of 20 mg/mL at pH = 2.5 at two temperatures of 20 and 40 °C, respectively. Red solid lines represent the experimental data, while dashed black lines show the fits. By calculating the areas of the absorption bands, we find that the ratio between −COO⁻ and −COOH is constant (∼1.1).

solution was prepared at a concentration of 40 mM of DCl in order to obtain a pH of 2.5 where hyaluronan is in the putty state, following the same protocol as previously described.[39] We observe three absorption bands at 1633, 1725, and 1609 cm⁻¹, which based on prior work[62] we assign to, respectively, the amide I vibration (AM.I), the carbonyl stretching mode of the protonated carboxylic acid group (C=O), and the antisymmetric stretch vibration of the carboxylate group anion group (COO_{ant}^-). The relative intensities of the C=O and COO_{ant}^- bands directly reflect the protonation state of hyaluronan.[39] Using the procedure described in the Experimental Section, we determined the absorption band areas. We thus find that the fraction of deprotonated carboxyl groups (−COO⁻) is the same at 20 and at 40 °C. From the acid−base equilibrium of hyaluronan, we calculate that ∼20/30% of the −COO⁻ is deprotonated at pH 2.5.

To measure the density of hydrogen bonds as a function of temperature, we performed 2DIR spectroscopy measurements on hyaluronan solutions in D_2O at pH = 2.5 at several temperatures between 5 and 40 °C (Figure 4). We excited the amide and carboxyl vibrations with a strong ∼100 femtosecond infrared pulse pair centered at 1670 cm⁻¹. We probed the resulting transient absorption changes with a weaker (0.35 μJ) single femtosecond probing pulse that was delayed by a waiting time T_w (Figure 4a). Figure 4b,c shows the isotropic 2DIR spectra at the two temperature extremes of 5 and 40 °C. In both spectra, we observe on the diagonal four distinct spectral signatures. The blue-colored signatures represent negative absorption changes (which we refer to as *bleach*) that originate from a reduction of the absorption at the amide I and carboxyl carbonyl frequencies. This reduced absorption is due to the depletion of the fundamental transition ($v = 0$ to $v = 1$) and stimulated emission ($v = 1$ to $v = 0$) of the excited amide I and carbonyl vibrations. At somewhat lower probing frequencies, we observe red-colored spectral signatures, which represent positive absorption changes. These positive absorption changes can be assigned to excited-state absorption or *esa* and arise because of the vibrational transition from $v = 1$ to $v = 2$.[63] The
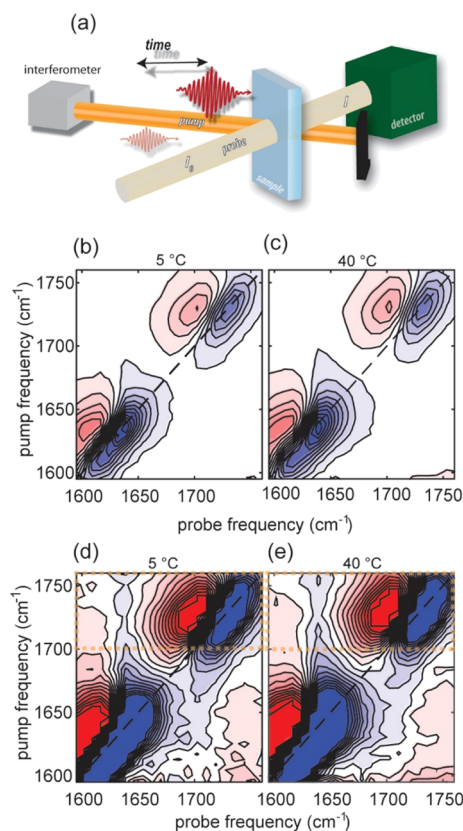

Figure 4. (a) Schematic of the 2DIR experiment (see main text for details). (b,c) 2DIR spectra of hyaluronan (20 mg/mL) at pH = 2.5 at a time delay T_w = 0.3 ps at two temperatures, namely, 5 (b) and 40 °C (c). Color code: from 1.5 a.u. (dark red) to −1.5 a.u. (dark blue) (b), from 0.75 a.u. (dark red) to −0.75 a.u. (dark blue). (d,e) Same spectra with color-bar fivefold magnified to show the presence of off-diagonal peaks in the frequency regions indicated by the orange dashed rectangles.

two pairs of diagonal peaks are obtained by exciting at 1633 and 1725 cm⁻¹, corresponding to the vibrational frequencies of the amide I and C=O absorption bands, respectively. The lower-frequency diagonal peak shows a shoulder at 1610 cm⁻¹, which we assign to the antisymmetric stretch vibration of the carboxylate anion.

When we multiply the 2DIR spectra by a factor of 5, we can also observe off-diagonal spectral signatures in the 2DIR spectrum at both temperatures (Figure 4d,e). The off-diagonal peaks are 10-fold weaker than the diagonal signals. In the top-left off-diagonal region (exciting around 1725 cm⁻¹ and probing around 1630 cm⁻¹), which is indicated by the orange-colored rectangle, we observe a 2DIR absorption signal associated with the excitation of the carbonyl vibration and probing of the amide I absorption. This off-diagonal feature is commonly referred to as a downhill cross-peak. Figure 5a reports the 2DIR signals obtained by averaging over the excitation frequencies between 1700 and 1760 cm⁻¹ (orange rectangle in Figure 4d,e). At each temperature, the 2DIR signal is normalized to the maximum intensity of the carbonyl bleach. In Figure 5a, we observe again the bleach and the esa of the carbonyl around 1700 cm⁻¹ and a negative 2DIR signal near 1635 cm⁻¹, which is the absorption frequency of the amide I vibration. The cross-peak signal between the carbonyl stretching and the amide I vibrations reveals the existence of molecular coupling between these groups at pH = 2.5 and
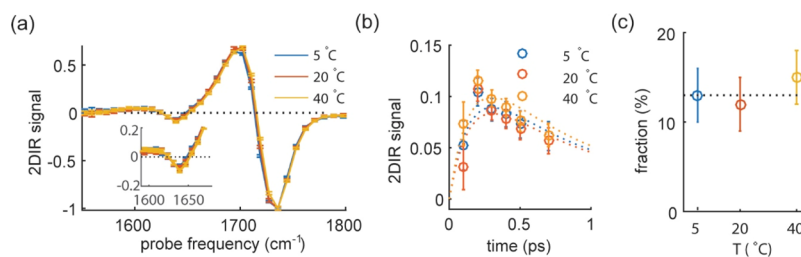
Figure 5. Temperature dependence of 2DIR spectral features for hyaluronan hydrogels at pH = 2.5. (a) 2DIR signals at three different temperatures obtained by averaging over the pump region between 1700 and 1760 cm^{-1}. Inset: details of the 2DIR signal in the absorption frequency of the amide I vibration showing the cross-peak signal is independent of temperature. (b) Cross-peak decay traces at 5, 20, and 40 °C. Dashed lines are fits to the relaxation model described in the main text. (c) Fraction of hydrogen-bonded carboxylic acid groups extracted from the 2DIR data is independent of temperature.

shows that a fraction of the carboxyl and the amide I groups are connected by a hydrogen bond.

To extract the fraction of hydrogen-bonded carboxyl and amide I groups, we consider the delay-time traces of the cross-peak signals shown in Figure 5b, obtained by fitting the 2DIR signals reported in Figure 5a (see the Methods section in the Supporting Information for details). The three delay-time traces are very similar, not showing a significant change upon changing the temperature. In order to extract the fraction of the hydrogen-bonded carboxyl and amide I groups at different temperatures, we analyzed the delay-time traces. In an earlier 2DIR study of hyaluronan,[39] we showed that upon excitation, the carbonyl stretching mode can relax following two different relaxation paths.

A fraction of the excited C=O vibrations relaxes by fast energy transfer to the amide I vibration with a time constant T_{ent} (~0.150 ps). This fast relaxation is enabled by the formation of the intermolecular hydrogen bonds. This energy-transfer process leads to excitation of the amide I vibration and thus to a fast rise of the cross-peak signal. Subsequently, the amide I mode relaxes back to the ground state with a time constant $T_{1AM.I}$ (~0.65 ps). Another fraction of the excited C=O groups is not hydrogen-bonded to an amide group and relaxes to low-frequency modes of the solvent or the hyaluronan polymer chain. This process is much slower and occurs with a time constant T_{1COOD} (~0.7 ps). Once populated, the low-frequency modes affect the absorption spectrum of the amide I vibration and also generate a 2DIR cross-peak signal. This latter contribution to the signal decays with a time constant T_{1LFM}, which is the relaxation time of the low-frequency modes. In our previous work,[39] we found that T_{1LFM} is ~3 ps, which is much slower than the decay of the amide I and C=O vibrations. Because the two relaxation mechanisms that determine the cross-peak dynamics occur on quite different time scales, they can be distinguished in a fit of the cross-peak delay-time traces with the following expression:

$$\frac{\Delta\alpha_{CP}(T_w)}{\Delta\alpha_{COOD}(T_w)} = c_{anh}\left(\frac{T_{1LFM}}{T_{1COOD} - T_{1LFM}}\right)(e^{-T_w/T_{1COOD}}$$

$$- e^{-T_w/T_{1LFM}}) + c_{ent}\left(\frac{T_{1AM.I}}{T_{ent} - T_{1AM.I}}\right)$$

$$(e^{-T_w/T_{ent}} - e^{-T_w/T_{1AM.I}}) \qquad (4)$$

where $\Delta\alpha_{CP}(T_w)/\Delta\alpha_{COOD}(\overline{T_w})$ is the intensity of the cross-peak normalized to the intensity of the C=O vibration at early time delay and $\overline{T_w}$ = 200 fs. The parameters c_{anh} and c_{ent} represent the cross-peak amplitudes associated with the

anharmonic coupling and direct energy-transfer mechanisms, respectively, and are the only free parameters. Because of the limited amount of data points at long time delay, the value of c_{anh} is constrained to be at least 0.02, which is the minimum value expected for this parameter based on our previous work (c_{anh} = 0.025 ± 0.005). Hence, we extract the amplitude of the fast relaxation component because of energy transfer, which can be directly linked to the fraction of protonated carboxylic acid bonded to the amide groups. We find that around 15% of the carbonyl groups are hydrogen-bonded to the amide groups at pH = 2.5 (Figure 5C), which closely agrees with our previous findings from 2DIR spectroscopy.[39] The requirement to alternate a double bond between a −COOH and amide with a single bond between −COO$^-$ and amide (as observed in Figure 1a) strongly limits the fraction of carboxylic acid groups that sterically can form a double hydrogen bond with an amide group. As shown in Figure 5c, we also observed that this fraction does not change in the temperature interval between 5 and 40 °C, which indicates that for these carboxylic acid groups the free energy of a configuration with a double hydrogen bond to an amide group is similar to the free energy of a configuration in which the carboxylic acid group is hydrogen-bonded to water molecules. This would mean that the total fraction of carboxylic acid groups that sterically can engage in a double hydrogen bond with an amide group is ~30%.

Connection between Rheology and 2DIR. The 2DIR measurements show that the fraction of carboxyl groups that are engaged in a direct hydrogen bond with an amide group does not change with temperature between 5 and 40 °C. This finding is consistent with the TTS analysis of the rheology data, which showed that the density of stickers that impede stress relaxation also does not change with temperature. These findings indicate that the breaking of an interchain hydrogen bond between a carboxyl group and an amide group results in a state that has about the same overall free energy as the intact hydrogen bond (see schematic in Figure 6). This other state is probably formed by hydrogen bonds between the carboxyl and the amide groups and solvent molecules. As a result, a change in temperature does not affect the number of hydrogen bonds that are formed between the polymer chains. However, the kinetics do change with temperature, as the breaking and reformation involves an energy barrier $E_{A,hb}$ that will be of the order of the binding energy of a single hydrogen bond, which is typically ~400−1400 cm^{-1} or 2−7 k_BT (T = 298 K).[64,65]

To understand the acceleration of the network dynamics with increasing temperature, we need to find the relation between the characteristic lifetime of a single hydrogen bond τ
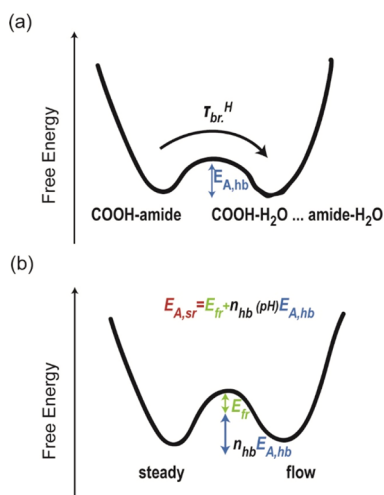
Figure 6. (a) Schematic representation of the breaking of a hydrogen-bonded complex. We refer to the breakage time of the hydrogen bonds as τ_{br}^H. The activation energy necessary to break the hydrogen-bonded complex is defined as $E_{A,hb}$. (b) Schematic representation of the network dynamics. The flow activation energy $E_{A,sr}$ corresponds to the breaking of n_{hb} hydrogen bonds (stickers).

and the characteristic time scale of the stress relaxation of the hyaluronan solution, as expressed in the frequency dependence of the shear moduli. The typical lifetime $\tau = \tau_{br}^H$ of a single hydrogen bond is on the order of a few to tens of picoseconds.[36] This large disparity in time scales between single hydrogen bond dynamics and sticker dynamics can be understood from the fact that multiple hydrogen bonds n_{hb} need to be broken at the same time to allow for chain displacement and thus flow of the network. In addition, such a mesoscopic rearrangement involves a frictional barrier E_{fr} because of chain entanglements and viscous drag with the solvent. Hence, the activation energy necessary for the network to flow will be larger than the activation energy of breaking a single hydrogen bond. Assuming a similar pre-exponential (Arrhenius) prefactor for the breaking of hydrogen bonds and the friction, the total activation energy for stress relaxation can be written as

$$E_{A,sr}(pH) = n_{hb}(pH)E_{A,hb} + E_{fr} \tag{5}$$

At pH = 7, we can assume that there are no hydrogen bonds ($n_{hb} = 0$) formed between the hyaluronan polymer chains based on earlier work showing that excluded volume interactions alone are enough to explain the concentration-dependent rheology.[37] Thus, the activation energy at pH 7 will be equal to the frictional barrier energy E_{fr}. At pH = 2.5, hydrogen bonds are formed between the hyaluronan polymer chains and their density is large enough to cause the formation of an elastic hydrogel. By subtracting the frictional energy E_{fr} from the activation energy measured at pH = 2.5, $E_{A,sr}$, we find that the energy barrier due to hydrogen bonds at pH 2.5 is around 85 kJ/mol ($\sim$38 k_BT). This residual activation energy corresponds to $n_{hb} = 5-15$ hydrogen bonds, which thus need to be broken in order for the hyaluronan chain to diffuse at pH = 2.5.

An alternative way to estimate the number of hydrogen bonds that need to be simultaneously dissociated to enable stress relaxation is to consider the number of hydrogen bonds belonging to the same Kuhn segment.[66] Based on previous literature,[67] the Kuhn length (L_k) of hyaluronan is $\sim$18 nm at

200 mM NaCl at neutral pH, which is consistent with the highest estimation reported in the literature for the persistence length ($L_p = 7-10$ nm)[33] assuming a worm-like chain model ($L_k = 2L_p$). In AFM measurements,[50] we recently measured a persistence length of $\sim$4 nm (and thus $L_k = 8$ nm) under similar conditions. Persistence length measurements at pH = 2.5 are unfortunately not available, but we expect a similar value because there is still a significant presence of negative charges at this pH. Assuming a Kuhn length of 8 nm, we estimate that $\sim$8 disaccharide units belong to the same L_k segment. Further, we previously demonstrated[39] that an alternation of COOH and COO$^-$ groups is necessary for the formation of a strong hydrogen-bond network (see Figure 1a of the article). Considering that from steric considerations, $\sim$30% of the carboxylic acid groups can form a hydrogen bond complex with an amide group on an adjacent chain and that half of these groups, that is, $\sim$15% of the total number of carboxylic acid groups, is actually involved in the hydrogen-bond formation, we find that per Kuhn's segment around one $-$COOH forms a double hydrogen bond with the amide group of a second chain, and similarly per Kuhn's segment around one amide group forms a double bond with the $-$COOH group of a second chain, leading to four hydrogen bonds per chain. Furthermore, per Kuhn's segment around two $-$COO$^-$ groups can form hydrogen bonds with the amide groups of a second chain, and similarly per Kuhn's segment around two amide groups can form hydrogen bonds with the $-$COO$^-$ groups of a second chain, leading to an additional four hydrogen bonds. We thus estimate that $\sim$8 hydrogen bonds can be formed per Kuhn's segment. This number agrees well with the estimated number of hydrogen bonds $n_{hb} \approx 5-15$ per transient cross-link, which we estimated from the flow activation energy.

Furthermore, from the plateau modulus and the polymer concentration, we estimated earlier that the number of active transient cross-links is 11$-$14. By assuming that every cross-link point is composed of 5$-$15 hydrogen bonds, as we infer from the activation enthalpy, we find that the total number of hydrogen bonds per chain n_{hb} is around 55$-$210. This estimate is consistent with the finding from the 2DIR measurements that the number of hydrogen bonds per chain is roughly 375$-$550, assuming that one single chain is composed by roughly 3750 units and that just 10$-$15% of these participate in hydrogen-bond formation. We conclude that the number of hydrogen bonds that we estimated from the 2DIR data is consistent with the corresponding number extracted from the rheology data.

Finally, it should be noted that we have not considered the possible effect of temperature on the frictional energy barrier E_{fr}. This energy barrier will depend on several parameters, such as the intramolecular hydrogen bonds that stiffen hyaluronan and the mobility of the solvent molecules. Increased chain flexibility and water mobility could potentially lower E_{fr} as the temperature increases.[68,69] However, the fact that the temperature dependence of the shift factor a_T can be well described with an Arrhenius expression suggests that the value of E_{fr} is quite insensitive to temperature changes within the range (5$-$40 °C) we studied.

■ CONCLUSIONS

We used rheological and 2DIR spectroscopy measurements to measure the effect of temperature and pH on the mechanical properties and underlying molecular interactions of entangled

hyaluronan polymers. The rheology results showed that changing the pH from 7.0 to 2.5 introduces associative interactions that strongly slow down stress relaxation. The 2DIR results showed that these associative interactions are mediated by hydrogen bonds whose equilibrium density does not depend on the temperature (from 5 to 40 °C) but only on pH. Hence, the equilibrium structure of the hyaluronan polymer network does not change with temperature. The kinetics of the polymer network does show a strong dependence on temperature. By performing measurements over an extended temperature range (5−40 °C), we could show that the stress relaxation time displays an Arrhenius-type dependence on temperature with a flow activation energy of 12 k_BT (~30 kJ/mol) at pH 7.0 and 50 k_BT (~115 kJ/mol) at pH 2.5. The activation energy at pH 7.0 can be assigned to a frictional energy barrier associated with the motion of the polymer chains along each other and the displacement of water molecules. The much higher activation energy at pH = 2.5 indicates that under these conditions, the simultaneous breaking of 5−15 hydrogen bonds is required for chains to move and, thus, for the network to flow. Our findings show that hyaluronan forms thermoreversible gels whose macroscopic properties can be tuned by pH and temperature.

In the context of human physiology, understanding how the mechanical properties of extracellular glycosaminoglycans such as hyaluronan are affected by pH is relevant because many diseases, such as cancer and inflammation, are associated with acidosis, a decrease of the extracellular pH.[70−72] Even though the average pH values in this situation are reported to be of order 5.8 [ref 73], potentially lower pH values might be reached locally and transiently, which may strongly affect the dynamics of the hyaluronan polymer network. Moreover, pH-responsive hydrogels may potentially serve for targeted release of anticancer drugs.[74] In the context of materials science, it has become clear in recent years that noncovalently bonded hydrogels have many desirable properties such as stimulus-responsiveness, toughness, and an inherent capacity for self-healing and recovery after mechanical damage. Such materials have possible applications for shape memory, self-healing, and adhesive materials.[1] Hyaluronan is biocompatible and already used for a broad range of biomedical applications, from drug delivery to tissue regeneration.[7,8,75] It would therefore be interesting to extend our study of the linear rheological properties of hyaluronan hydrogels in the future to the nonlinear regime of large deformations and to complex time-dependent effects such as plasticity and self-healing.[76]

■ ASSOCIATED CONTENT

Ⓢ Supporting Information

The Supporting Information is available free of charge at https://pubs.acs.org/doi/10.1021/acs.macromol.0c01742.

> Fitting procedure of the transient absorption spectra and the relaxation model and thermoreversibility of the rheology of hyaluronan and the concentration dependence of the flow activation energies (PDF)

■ AUTHOR INFORMATION

Corresponding Authors

Gijsje H. Koenderink − *AMOLF, Amsterdam 1098 XG, The Netherlands; Department of Bionanoscience, Kavli Institute of Nanoscience Delft, Delft University of Technology, Delft 2629 HZ, The Netherlands;* ⓞ orcid.org/0000-0002-7823-8807; Email: g.h.koenderink@tudelft.nl

Huib J. Bakker − *AMOLF, Amsterdam 1098 XG, The Netherlands;* ⓞ orcid.org/0000-0003-1564-5314; Email: h.bakker@amolf.nl

Authors

Giulia Giubertoni − *AMOLF, Amsterdam 1098 XG, The Netherlands;* ⓞ orcid.org/0000-0002-3417-4987

Federica Burla − *AMOLF, Amsterdam 1098 XG, The Netherlands*

Complete contact information is available at:
https://pubs.acs.org/10.1021/acs.macromol.0c01742

Notes

The authors declare no competing financial interest.

■ REFERENCES

(1) Cohen Stuart, M. A.; Huck, W. T. S.; Genzer, J.; Müller, M.; Ober, C.; Stamm, M.; Sukhorukov, G. B.; Szleifer, I.; Tsukruk, V. V.; Urban, M.; Winnik, F.; Zauscher, S.; Luzinov, I.; Minko, S. Emerging applications of stimuli-responsive polymer materials. *Nat. Mater.* **2010**, *9*, 101−113.

(2) Zhang, Z.; Chen, Q.; Colby, R. H. Dynamics of associative polymers. *Soft Matter* **2018**, *14*, 2961−2977.

(3) Hofman, A. H.; van Hees, I. A.; Yang, J.; Kamperman, M. Bioinspired Underwater Adhesives by Using the Supramolecular Toolbox. *Adv. Mater.* **2018**, *30*, 1704640.

(4) Li, J.; Mooney, D. J. Designing hydrogels for controlled drug delivery. *Nat. Rev. Mater.* **2016**, *1*, 16071.

(5) Rosales, A. M.; Anseth, K. S. The design of reversible hydrogels to capture extracellular matrix dynamics. *Nat. Rev. Mater.* **2016**, *1*, 15012.

(6) Stanton, M. M.; Samitier, J.; Sánchez, S. Bioprinting of 3D hydrogels. *Lab-on-a-Chip* **2015**, *15*, 3111−3115.

(7) Highley, C. B.; Prestwich, G. D.; Burdick, J. A. Recent advances in hyaluronic acid hydrogels for biomedical applications. *Curr. Opin. Biotechnol.* **2016**, *40*, 35−40.

(8) Wolf, K. J.; Kumar, S. Hyaluronic Acid: Incorporating the Bio into the Material. *ACS Biomater. Sci. Eng.* **2019**, *5*, 3753−3765.

(9) Geissler, E.; Hecht, A. M.; Horkay, F. Scaling equations for a biopolymer in salt solution. *Phys. Rev. Lett.* **2007**, *99*, 267801.

(10) Berezney, J. P.; Saleh, O. A. Electrostatic effects on the conformation and elasticity of hyaluronic acid, a moderately flexible polyelectrolyte. *Macromolecules* **2017**, *50*, 1085−1089.

(11) Lee, J. Y.; Spicer, A. P. Hyaluronan: a multifunctional, megaDalton, stealth molecule. *Curr. Opin. Cell Biol.* **2000**, *12*, 581−586.

(12) Horkay, F.; Basser, P. J.; Londono, D. J.; Hecht, A.-M.; Geissler, E. Ions in hyaluronic acid solutions. *J. Chem. Phys.* **2009**, *131*, 184902.

(13) Horkay, F.; Magda, J.; Alcoutlabi, M.; Atzet, S.; Zarembinski, T. Structural, mechanical and osmotic properties of injectable hyaluronan-based composite hydrogels. *Polymer* **2010**, *51*, 4424−4430.

(14) Cowman, M. K.; Schmidt, T. A.; Raghavan, P.; Stecco, A. Viscoelastic properties of hyaluronan in physiological conditions. *F1000Research* **2015**, *4*, 622.

(15) Zhu, Y.; Granick, S. Biolubrication: Hyaluronic Acid and the Influence on Its Interfacial Viscosity of an Antiinflammatory Drug. *Macromolecules* **2003**, *36*, 973−976.

(16) Shenoy, V.; Rosenblatt, J. Diffusion of macromolecules in collagen and hyaluronic acid, rigid-rod-flexible polymer, composite matrixes. *Macromolecules* **1995**, *28*, 8751−8758.

(17) Richter, R. P.; Baranova, N. S.; Day, A. J.; Kwok, J. C. Glycosaminoglycans in extracellular matrix organisation: are concepts from soft matter physics key to understanding the formation of perineuronal nets? *Curr. Opin. Struct. Biol.* **2018**, *50*, 65−74.

(18) Kuo, J. C.-H.; Gandhi, J. G.; Zia, R. N.; Paszek, M. J. Physical biology of the cancer cell glycocalyx. *Nat. Phys.* **2018**, *14*, 658−669.

(19) Neuman, M. G.; Nanau, R. M.; Oruña-Sanchez, L.; Coto, G. Hyaluronic acid and wound healing. *J. Pharm. Pharm. Sci.* **2015**, *18*, 53−60.

(20) Rooney, P.; Kumar, S. Inverse relationship between hyaluronan and collagens in development and angiogenesis. *Differentiation* **1993**, *54*, 1−9.

(21) Petrey, A. C.; de la Motte, C. A. Hyaluronan, a crucial regulator of inflammation. *Front. Immunol.* **2014**, *5*, 101.

(22) Back, S. A.; Tuohy, T. M. F.; Chen, H.; Wallingford, N.; Craig, A.; Struve, J.; Luo, N. L.; Banine, F.; Liu, Y.; Chang, A.; Trapp, B. D.; Bebo, B. F., Jr.; Rao, M. S.; Sherman, L. S. Hyaluronan accumulates in demyelinated lesions and inhibits oligodendrocyte progenitor maturation. *Nat. Med.* **2005**, *11*, 966−972.

(23) Liu, M.; Tolg, C.; Turley, E. Dissecting the Dual Nature of Hyaluronan in the Tumor Microenvironment. *Front. Immunol.* **2019**, *10*, 947.

(24) Rankin, K. S.; Frankel, D. Hyaluronan in cancer - from the naked mole rat to nanoparticle therapy. *Soft Matter* **2016**, *12*, 3841−3848.

(25) Temple-Wong, M. M.; Ren, S.; Quach, P.; Hansen, B. C.; Chen, A. C.; Hasegawa, A.; D'Lima, D. D.; Koziol, J.; Masuda, K.; Lotz, M. K.; Sah, R. L. Hyaluronan concentration and size distribution in human knee synovial fluid: variations with age and cartilage degeneration. *Arthritis Res. Ther.* **2016**, *18*, 18.

(26) Gribbon, P.; Heng, B. C.; Hardingham, T. E. The molecular basis of the solution properties of hyaluronan investigated by confocal fluorescence recovery after photobleaching. *Biophys. J.* **1999**, *77*, 2210−2216.

(27) Innes-Gold, S. N.; Pincus, P. A.; Stevens, M. J.; Saleh, O. A. Polyelectrolyte Conformation Controlled by a Trivalent-Rich Ion Jacket. *Phys. Rev. Lett.* **2019**, *123*, 187801.

(28) Gibbs, D. A.; Merrill, E. W.; Smith, K. A.; Balazs, E. A. Rheology of hyaluronic acid. *Biopolymers* **1968**, *6*, 777−791.

(29) Gatej, I.; Popa, M.; Rinaudo, M. Role of the pH on hyaluronan behavior in aqueous solution. *Biomacromolecules* **2005**, *6*, 61−67.

(30) Wu, S.; Ai, L.; Chen, J.; Kang, J.; Cui, S. W. Study of the mechanism of formation of hyaluronan putty at pH 2.5: part I. Experimental measurements. *Carbohydr. Polym.* **2013**, *98*, 1677−1682.

(31) Wu, S.; Ai, L.; Chen, J.; Kang, J.; Cui, S. W. Study of the mechanism of formation of hyaluronan putty at pH 2.5: Part II-Theoretical analysis. *Carbohydr. Polym.* **2013**, *98*, 1683−1688.

(32) Balazs, E. A.; Cui, J. The story of "Hyaluronan Putty". *Bioact. Carbohydr. Diet. Fibre* **2013**, *2*, 143−151.

(33) Giubertoni, G.; Koenderink, G. H.; Bakker, H. J. Direct Observation of Intrachain Hydrogen Bonds in Aqueous Hyaluronan. *J. Phys. Chem. A* **2019**, *123*, 8220−8225.

(34) Leibler, L.; Rubinstein, M.; Colby, R. H. Dynamics of reversible networks. *Macromolecules* **1991**, *24*, 4701−4707.

(35) Rubinstein, M.; Semenov, A. N. Dynamics of entangled solutions of associating polymers. *Macromolecules* **2001**, *34*, 1058−1068.

(36) Woutersen, S.; Mu, Y.; Stock, G.; Hamm, P. Hydrogen-bond lifetime measured by time-resolved 2D-IR spectroscopy: N-methyl-acetamide in methanol. *Chem. Phys.* **2001**, *266*, 137−147.

(37) Krause, W. E.; Bellomo, E. G.; Colby, R. H. Rheology of sodium hyaluronate under physiological conditions. *Biomacromolecules* **2001**, *2*, 65−69.

(38) Charlot, A.; Auzély-Velty, R. Novel hyaluronic acid based supramolecular assemblies stabilized by multivalent specific interactions: rheological behavior in aqueous solution. *Macromolecules* **2007**, *40*, 9555−9563.

(39) Giubertoni, G.; Burla, F.; Martinez-Torres, C.; Dutta, B.; Pletikapic, G.; Pelan, E.; Rezus, Y. L. A.; Koenderink, G. H.; Bakker, H. J. Molecular Origin of the Elastic State of Aqueous Hyaluronic Acid. *J. Phys. Chem. B* **2019**, *123*, 3043−3049.

(40) Ahmadi, M.; Hawke, L. G. D.; Goldansaz, H.; van Ruymbeke, E. Dynamics of Entangled Linear Supramolecular Chains with Sticky Side Groups: Influence of Hindered Fluctuations. *Macromolecules* **2015**, *48*, 7300−7310.

(41) Hackelbusch, S.; Rossow, T.; van Assenbergh, P.; Seiffert, S. Chain Dynamics in Supramolecular Polymer Networks. *Macromolecules* **2013**, *46*, 6273−6286.

(42) Cyphert, J. M.; Trempus, C. S.; Garantziotis, S. Size Matters: Molecular Weight Specificity of Hyaluronan Effects in Cell Biology. *Int. J. Cell Biol.* **2015**, *2015*, 563818.

(43) Maxa, J. J.; Chapados, C. Isotope effects in liquid water by infrared spectroscopy. III. H2O and D2O spectra from 6000 to 0 cm⁻¹. *J. Chem. Phys.* **2009**, *131*, 184505.

(44) Krezel, A.; Bal, W. A formula for correlating pKa values determined in D2O and H2O. *J. Inorg. Biochem.* **2004**, *98*, 161−166.

(45) Lowry, K. M.; Beavers, E. M. Thermal stability of sodium hyaluronate in aqueous solution. *J. Biomed. Mater. Res.* **1994**, *28*, 1239−1244.

(46) Amunson, K. E.; Kubelka, J. On the temperature dependence of amide I frequencies of peptides in solution. *J. Phys. Chem. B* **2007**, *111*, 9993−9998.

(47) Selig, O.; Siffels, R.; Rezus, Y. L. Ultrasensitive Ultrafast Vibrational Spectroscopy Employing the Near Field of Gold Nanoantennas. *Phys. Rev. Lett.* **2015**, *114*, 233004.

(48) Blundell, C. D.; Deangelis, P. L.; Almond, A. Hyaluronan: the absence of amide-carboxylate hydrogen bonds and the chain conformation in aqueous solution are incompatible with stable secondary and tertiary structure models. *Biochem. J.* **2006**, *396*, 487−498.

(49) Attili, S.; Borisov, O. V.; Richter, R. P. Films of end-grafted hyaluronan are a prototype of a brush of a strongly charged, semiflexible polyelectrolyte with intrinsic excluded volume. *Biomacromolecules* **2012**, *13*, 1466−1477.

(50) Giubertoni, G.; Pérez de Alba Ortíz, A.; Bano, F.; Zhang, X.; Linhardt, R. J.; Green, D. E.; DeAngelis, P. L.; Koenderink, G. H.; Richter, R. P.; Ensing, B.; Bakker, H. J. Strong reduction of the chain rigidity of hyaluronan by selective binding of Ca²⁺ ions. **2020**, bioRxiv:2020.09.01.277194v1.

(51) Almond, A.; Deangelis, P. L.; Blundell, C. D. Hyaluronan: the local solution conformation determined by NMR and computer modeling is close to a contracted left-handed 4-fold helix. *J. Mol. Biol.* **2006**, *358*, 1256−1269.

(52) Almond, A.; Brass, A.; Sheehan, J. K. Oligosaccharides as Model Systems for Understanding Water−Biopolymer Interaction: Hydrated Dynamics of a Hyaluronan Decamer. *J. Phys. Chem. B* **2000**, *104*, 5634−5640.

(53) Dea, I. C. M.; Moorhouse, R.; Rees, D. A.; Arnott, S.; Guss, J. M.; Balazs, E. A. Hyaluronic acid: a novel, double helical molecule. *Science* **1973**, *179*, 560−562.

(54) Lodge, T. P.; Rotstein, N. A.; Prager, S. Dynamics of entangled polymer liquids. Do linear chains reptate?. *Advances in Chemical Physics*: Wiley, 1990; Vol. 79, pp 1−132.

(55) Dodero, A.; Williams, R.; Gagliardi, S.; Vicini, S.; Alloisio, M.; Castellano, M. A micro-rheological and rheological study of biopolymers solutions: Hyaluronic acid. *Carbohydr. Polym.* **2019**, *203*, 349−355.

(56) Oelschlaeger, C.; Cota Pinto Coelho, M.; Willenbacher, N. Chain flexibility and dynamics of polysaccharide hyaluronan in

entangled solutions: a high frequency rheology and diffusing wave spectroscopy study. *Biomacromolecules* **2013**, *14*, 3689−3696.

(57) Dougherty, R. C. Temperature and pressure dependence of hydrogen bond strength: A perturbation molecular orbital approach. *J. Chem. Phys.* **1998**, *109*, 7372.

(58) Tanaka, F.; Edwards, S. F. Viscoelastic properties of physically crosslinked networks. *J. Non-Newtonian Fluid Mech.* **1992**, *43*, 273−288.

(59) Ferry, J. D. *Viscoelastic Properties of Polymers*; John Wiley & Sons: New York, 1980.

(60) Shamoun, R. F.; Hariri, H. H.; Ghostine, R. A.; Schlenoff, J. B. Thermal transformations in extruded saloplastic polyelectrolyte complexes. *Macromolecules* **2012**, *45*, 9759−9767.

(61) Spruijt, E.; Sprakel, J.; Lemmers, M.; Stuart, M. A.; van der Gucht, J. Relaxation dynamics at different time scales in electrostatic complexes: time-salt superposition. *Phys. Rev. Lett.* **2010**, *105*, 208301.

(62) Kovács, A.; Nyerges, B.; Izvekov, V. Vibrational analysis of N-acetyl-alpha-D-glucosamine and beta-D-glucuronic acid. *J. Phys. Chem. B* **2008**, *112*, 5728−5735.

(63) Hamm, P.; Zanni, M. *Concepts and Methods of 2D Infrared Spectroscopy*; Cambridge University Press: Cambridge, 2011; pp 636.

(64) Sheu, S.-Y.; Yang, D.-Y.; Selzle, H. L.; Schlag, E. W. Energetics of hydrogen bonds in peptides. *Proc. Natl. Acad. Sci. U.S.A.* **2003**, *100*, 12683−12687.

(65) Bolen, D. W.; Rose, G. D. Structure and energetics of the hydrogen-bonded backbone in protein folding. *Annu. Rev. Biochem.* **2008**, *77*, 339−362.

(66) Hamad, F. G.; Chen, Q.; Colby, R. H. Linear Viscoelasticity and Swelling of Polyelectrolyte Complex Coacervates. *Macromolecules* **2018**, *51*, 5547−5555.

(67) Reed, C. E.; Li, X.; Reed, W. F. The effects of pH on hyaluronate as observed by light scattering. *Biopolymers* **1989**, *28*, 1981−2000.

(68) Tarek, M.; Tobias, D. J. Role of protein-water hydrogen bond dynamics in the protein dynamical transition. *Phys. Rev. Lett.* **2002**, *88*, 138101.

(69) Giannotti, M. I.; Rinaudo, M.; Vancso, G. J. Force spectroscopy of hyaluronan by atomic force microscopy: from hydrogen-bonded networks toward single-chain behavior. *Biomacromolecules* **2007**, *8*, 2648−2652.

(70) Gerweck, L. E.; Seetharaman, K. Cellular pH gradient in tumor versus normal tissue: potential exploitation for the treatment of cancer. *Cancer Res.* **1996**, *56*, 1194−1198.

(71) Corbet, C.; Feron, O. Tumour acidosis: from the passenger to the driver's seat. *Nat. Rev. Cancer* **2017**, *17*, 577−593.

(72) Erra Díaz, F.; Ochoa, V.; Merlotti, A.; Dantas, E.; Mazzitelli, I.; Gonzalez Polo, V.; Sabatté, J.; Amigorena, S.; Segura, E.; Geffner, J. Extracellular Acidosis and mTOR Inhibition Drive the Differentiation of Human Monocyte-Derived Dendritic Cells. *Cell Rep.* **2020**, *31*, 107613.

(73) Erra Díaz, F.; Dantas, E.; Geffner, J. Unravelling the Interplay between Extracellular Acidosis and Immune Cells. *Mediators Inflammation* **2018**, *2018*, 1218297.

(74) Schmaljohann, D. Thermo- and pH-responsive polymers in drug delivery☆. *Adv. Drug Delivery Rev.* **2006**, *58*, 1655−1670.

(75) Singh, A.; Corvelli, M.; Unterman, S. A.; Wepasnick, K. A.; McDonnell, P.; Elisseeff, J. H. Enhanced lubrication on tissue and biomaterial surfaces through peptide-mediated binding of hyaluronic acid. *Nat. Mater.* **2014**, *13*, 988−995.

(76) Meng, F.; Pritchard, R. H.; Terentjev, E. M. Stress Relaxation, Dynamics, and Plasticity of Transient Polymer Networks. *Macromolecules* **2016**, *49*, 2843−2852.